

## RESEARCH ARTICLE

# Local fat content determines global and local stiffness in livers with simple steatosis

David Li<sup>1,2</sup>  | Paul A. Janmey<sup>2,3,4,5</sup> | Rebecca G. Wells<sup>1,2,3</sup> 

<sup>1</sup>Division of Gastroenterology and Hepatology, Department of Medicine, University of Pennsylvania, Philadelphia, Pennsylvania, USA

<sup>2</sup>NSF Science and Technology Center for Engineering MechanoBiology, University of Pennsylvania, Philadelphia, Pennsylvania, USA

<sup>3</sup>Department of Bioengineering, University of Pennsylvania, Philadelphia, Pennsylvania, USA

<sup>4</sup>Institute for Medicine and Engineering, University of Pennsylvania, Philadelphia, Pennsylvania, USA

<sup>5</sup>Department of Physiology, University of Pennsylvania, Philadelphia, Pennsylvania, USA

## Correspondence

Rebecca G. Wells, 905 BRB II/III, 421 Curie Boulevard, Philadelphia, PA 19104-6140, USA.  
Email: [rgwells@penmedicine.upenn.edu](mailto:rgwells@penmedicine.upenn.edu)

## Funding information

National Institutes of Health, Grant/Award Number: R01EB017753; Center for Engineering MechanoBiology (CEMB); NSF Science and Technology Center, Grant/Award Number: CMMI1548571

## Abstract

Fat accumulation during liver steatosis precedes inflammation and fibrosis in fatty liver diseases, and is associated with disease progression. Despite a large body of evidence that liver mechanics play a major role in liver disease progression, the effect of fat accumulation by itself on liver mechanics remains unclear. Thus, we conducted ex vivo studies of liver mechanics in rodent models of simple steatosis to isolate and examine the mechanical effects of intrahepatic fat accumulation, and found that fat accumulation softens the liver. Using a novel adaptation of microindentation to permit association of local mechanics with microarchitectural features, we found evidence that the softening of fatty liver results from local softening of fatty regions rather than uniform softening of the liver. These results suggest that fat accumulation itself exerts a softening effect on liver tissue. This, along with the localized heterogeneity of softening within the liver, has implications in what mechanical mechanisms are involved in the progression of liver steatosis to more severe pathologies and disease. Finally, the ability to examine and associate local mechanics with microarchitectural features is potentially applicable to the study of the role of heterogeneous mechanical microenvironments in both other liver pathologies and other organ systems.

## KEYWORDS

fat, hepatocyte, NAFLD, rheology, steatosis, tissue mechanics

**Abbreviations:** DAPI, 4',6'-diamidino-2-phenylindole; MRE, magnetic resonance elastography; NAFLD, non-alcoholic fatty liver disease; NASH, non-alcoholic steatohepatitis.

This is an open access article under the terms of the [Creative Commons Attribution-NonCommercial](https://creativecommons.org/licenses/by-nc/4.0/) License, which permits use, distribution and reproduction in any medium, provided the original work is properly cited and is not used for commercial purposes.

©2023 The Authors *FASEB BioAdvances* published by The Federation of American Societies for Experimental Biology.

## 1 | INTRODUCTION

Liver steatosis is the accumulation of fat within the liver and is associated with progression to more severe pathologies including steatohepatitis, fibrosis, cirrhosis, and hepatocellular carcinoma.<sup>1,2</sup> Steatosis affects over 32% of adults in the United States<sup>3</sup> and is among the first pathological changes in both alcoholic and non-alcoholic fatty liver disease, preceding inflammation and fibrosis and often preceding symptoms.<sup>1,4,5</sup> As such, understanding the contributions of fat accumulation is critical to understanding the mechanisms involved in the development of fatty liver diseases at their earliest stages.

The effect of fat accumulation itself on disease progression in the absence of fibrosis or inflammation is, however, relatively poorly understood. In particular, despite the well-documented connection between liver stiffness and fibrosis,<sup>6–8</sup> the effect of isolated steatosis on the mechanical properties of the liver has yet to be defined. Previous investigations in other tissues have shown that fat accumulation in tissues alters tissue mechanics, but whether it exerts a softening or stiffening effect has been variable and tissue specific.<sup>9–12</sup> Most studies of liver mechanics during fatty liver disease have focused on later stages of the disease, during which inflammation and fibrotic remodeling may obscure the contribution of fat accumulation.<sup>12–14</sup> Furthermore, past work was largely carried out in vivo,<sup>15–19</sup> where changes in fluid pressure presented a confounding factor.<sup>20–22</sup> Thus, the impact of fat accumulation in isolation on liver mechanics is not known.

In addition, fatty liver disease is histologically heterogeneous at the sub-millimeter (meso) scale,<sup>4,23</sup> which is the scale most relevant to mechanosensing.<sup>24–26</sup> This local variation in fat accumulation may cause changes in the mechanical microenvironment of liver cells in ways distinct from that of whole organ mechanics. Due to limitations in methodology, previous work has been unable to link mesoscale architecture and mechanics in the fatty liver. The resolution of ultrasound-based methods such as transient elastography is poor at sub-millimeter scales,<sup>27,28</sup> while atomic force microscopy (AFM) is best at the nanoscale.<sup>29</sup> Microindentation provides accurate mechanical measurements at the relevant scale, but it has been difficult to correlate mechanics and architecture.<sup>29</sup> As a result, although there is histological evidence of local heterogeneity in fat accumulation in liver, how this heterogeneity affects the mechanical microenvironment at cell-relevant scales has not been explored.

In this work, we address these questions by determining the effects of simple steatosis, without inflammation or fibrosis, on the mechanics of both the whole liver and heterogeneous regions of fat accumulation within the tissue. Using the ob/ob mouse as a genetic model of simple

steatosis, we measured whole liver mechanics by rheometry. The liver was studied *ex vivo* to avoid confounding from fluid pressure. To determine whether local differences in fat accumulation cause local changes in tissue mechanics, we used a new method to measure local stiffness values by microindentation and to demarcate the measured regions for subsequent correlation with lipid droplet staining and other microarchitectural studies. With this new combined approach, we determined that fat accumulation softens the liver at both whole organ and meso scales. This may have important implications for understanding the progression of fatty liver disease.

## 2 | MATERIALS AND METHODS

### 2.1 | Animal studies

All animal work was carried out in strict accordance with the recommendations in the Guide for the Care and Use of Laboratory Animals of the National Institutes of Health. Animal protocols were approved by the Institutional Animal Care and Use Committee of the University of Pennsylvania (protocol #804031). Ob/ob mice were obtained from the Jackson Laboratories (strain #000632) and were housed in a temperature-controlled environment with appropriate enrichment, *ad libitum* feeding of standard rodent chow and water, and 12h light/dark cycles. Euthanasia was carried out by CO<sub>2</sub> inhalation followed by exsanguination. Whole livers were harvested from ob/ob mice and wild type littermates at 8, 12, and 36 weeks and stored in PBS at 4°C for up to 5h until just before being analyzed; rodent livers are adequately preserved under these conditions and rheological properties are maintained.<sup>30,31</sup>

### 2.2 | Tissue staining and quantification

Samples from each liver were snap frozen in OCT and sectioned with a cryostat before staining with 10 μM BODIPY 493/503 (D3922, Thermo Fisher) and 1 μg/mL DAPI (D1306, Thermo Fisher) for 30 min at room temperature. The degree of steatosis was quantified by measuring the area of BODIPY staining in multiple 500 × 500 μm regions randomly selected throughout the liver. Additional liver samples were formalin fixed and paraffin embedded before staining with either hematoxylin and eosin or picosirius red (S2365, Poly Scientific R&D Corp). Immunohistochemical staining was performed as described previously<sup>32</sup> with rabbit monoclonal anti-myeloperoxidase (MPO) antibody (1:1000, Abcam, Cat# ab208670, RRID: AB\_2864724) as the primary antibody.<sup>33</sup>

The degree of inflammation was quantified as the number of MPO-positive inflammatory cell foci in  $500 \times 500 \mu\text{m}$  regions randomly taken throughout the liver, while the degree of fibrosis was quantified by measuring the area of picrosirius red staining in multiple  $300 \times 300 \mu\text{m}$  regions between adjacent central veins and portal triads.

## 2.3 | Shear rheometry

Shear rheometry was performed as described previously.<sup>30</sup> Briefly, liver samples were prepared using an 8 mm punch (MP0144, Alabama R&D) with all punches taken in the same orientation from the same lobe. The height of the slices ranged from 2.0 to 3.9 mm in the uncompressed state. Samples were kept hydrated during all experiments with PBS. Parallel plate shear rheometry was carried out on a Kinexus PRO rheometer (Kinexus series, Malvern Instruments) at room temperature. Samples were attached to rheometer platforms with fibrin glue by applying  $5 \mu\text{L}$  each of 20 mg/mL bovine plasma fibrinogen (341,573, Sigma-Aldrich) and 100 U/mL bovine thrombin (T4648, Sigma-Aldrich) to both the top and bottom sides of the sample. The upper platen was quickly lowered until 0.02 N of nominal initial force was applied to ensure adhesive contact of the sample with the metal surfaces of the rheometer, and the sample was allowed to sit for 10 min to allow the fibrin glue to polymerize fully before performing measurements. The fibrin glue does not affect the mechanics of the system.<sup>30</sup> Mechanics were measured with a dynamic time sweep test (2% constant strain, oscillation frequency 1 rad/s, measurements taken for 120 s). These measurements were carried out first uncompressed, then with increasing uniaxial tension (10% and 20%), then uncompressed, then with increasing uniaxial compression (10, 15, 20, and 25%). Tension and compression were applied by changing the gap between the platform and upper platen of the rheometer. The following correction

was applied to account for the change in cross-sectional area during testing under the assumption that total tissue volume is conserved, where  $G'$  is the storage modulus and  $\lambda$  is axial strain:

$$G'_{\text{actual}} = G'_{\text{measured}}(1 + \lambda)^2$$

A similar correction was applied to the loss modulus  $G''$  and normal stress  $\delta$ . Young's modulus  $E$  was determined by calculating the slope of stress (Pa) versus axial strain.<sup>30</sup> Young's modulus  $E$  at zero compression was determined by the slope of stress versus axial strain between  $-10\%$  and  $10\%$  compression.

## 2.4 | Microindentation and demarcation of microindented regions

Microindentation was performed as described previously,<sup>29</sup> with additional modifications to permit the demarcation and visualization of mesoscale features within the microindented regions of the tissue (Figure 1). Briefly, the microindentation device consists of a stepping motor (L4018S1204-M6, Nanotec) attached to a  $\mu\text{N}$ -resolution tensiometric probe adapted from the surface tension measurement apparatus of a Langmuir monolayer trough (MicroTrough X, Kibron Inc.), consisting of a 0.510 mm diameter blunt-ended cylindrical tungsten alloy wire hung from a digital microbalance. The force-displacement relationship was found to behave as a Hookean spring with force linearly related to displacement, and the spring constant was calibrated before each measurement ( $k_{\text{probe}} \sim 4.5 \text{ N/m}$ ).

Liver samples 3 mm thick were prepared from liver tissue cores obtained using an 8 mm punch, removing the liver capsule. A ring of Parafilm was prepared using a 2 mm disposable biopsy punch and placed around a randomly selected region of interest on top of the liver sample. Samples were then manually positioned under

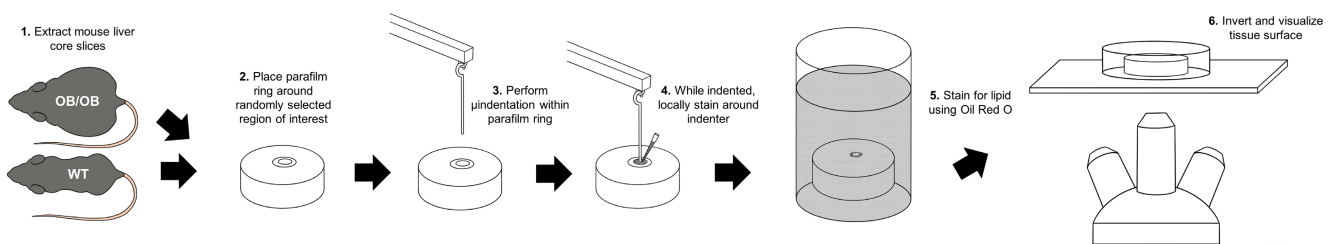


**FIGURE 1** Schematic of technique combining microindentation with visualization of tissue features. After removing livers from mice and generating liver core slices (step 1), parafilm rings were placed around randomly-selected regions of interest on each slice (step 2), and microindentation was performed on the region within each ring (step 3). After measuring local mechanics, the indenter was lowered to fully indent the microindented region and a stain was locally applied within the parafilm ring around the microindenter (step 4). Afterward, the tissue slices were stained for lipid using Oil red O (step 5) and inverted on an epifluorescent microscope to visualize lipid accumulation within each locally-stained region (step 6).

the free-hanging probe, followed by downward displacement of the probe until contact occurred between the probe and the sample in the center of the Parafilm ring. Following establishment of contact between probe and sample, the probe was translated downward at a continuous rate of 0.0125 mm/s. These translations resulted in decreases in measurable force from the probe, which were converted into local Young's modulus as described previously.<sup>29</sup> After the probe was fully indented into the sample (as determined by the absence of measurable force from the probe), 0.5  $\mu$ L of 100  $\mu$ g/mL DAPI (D1306, Invitrogen) solution was pipetted around the probe and allowed to selectively stain tissue within the Parafilm ring for 15 s before the sample was washed with PBS. Multiple measurements were obtained per liver sample using this approach. After microindentation and demarcation, liver samples were stored in PBS at 4°C for up to 5 h before being stained and imaged for lipid accumulation.

## 2.5 | Visualization and quantification of lipid accumulation of microindented regions

Liver samples were stained for lipid using an adaptation of whole mount Oil red O staining.<sup>34</sup> All incubation steps were performed at room temperature on a shaker. Briefly, samples were incubated with 0.5% Tween 20 (#170–6531, Bio-Rad) in PBS for 15 min, changing the solution every

5 min, before incubating with 0.5% Oil red O in propylene glycol (D1306, Poly Scientific R&D Corp) for 15 min. Afterward, the samples were washed once with Tween solution before incubating with Tween solution for 15 min, changing the solution every 5 min. Whole mount Oil red O staining of liver slices served as a rapid and easy technique to visualize the heterogeneous distribution of lipid on the surface of liver tissue samples (Figure 2A).

Visualization of lipid accumulation in microindented regions was performed using whole mount epifluorescence microscopy on a Nikon Eclipse Ti widefield microscope equipped with a 4x/0.31 N.A. PlanFluor dry objective lens and motorized stage. Lipid,<sup>35</sup> DAPI demarcation, and liver autofluorescence were visualized using Cy3, DAPI, and FITC filters, respectively. Using this approach, it was possible to visualize both the microindented regions and local lipid accumulation in the same regions (Figure 2B). Using autofluorescence, it was also possible to identify microscale anatomical features on the surface of the tissue such as intrahepatic blood vessels (Figure 2C). Quantification of lipid accumulation within demarcated DAPI rings was performed by simple thresholding of the Cy3 channel after shading correction in ImageJ.

## 2.6 | Statistical analysis

The statistical significance of differences between strain-dependent shear rheometry curves ( $G'$ ,  $G''$ , and  $E$ ) of ob/

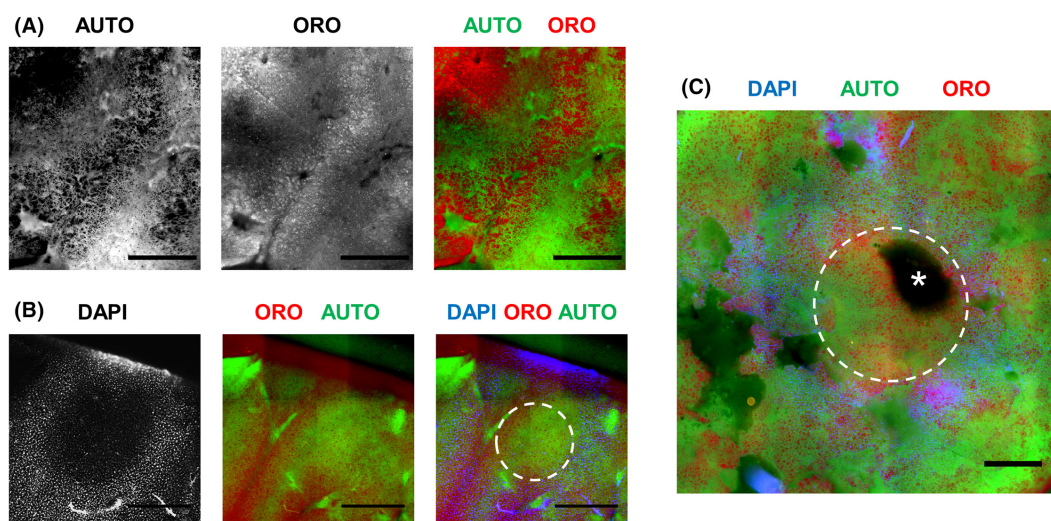


**FIGURE 2** Whole mount fluorescent staining and microscopy shows features of ob/ob livers. (A) Whole mount epifluorescence microscopy images of autofluorescence (left) and intracellular lipid accumulation in hepatocytes show spatial heterogeneity of lipid accumulation at the submillimeter scale of 12 weeks ob/ob livers. (B) Whole mount epifluorescence microscopy images of a 12 weeks wt liver showing DAPI (blue) demarcating the microindented region (left), autofluorescence (green), and heterogeneous lipid accumulation using Oil red O (red, middle), and the three channels merged (right) showing low lipid in the indented region (white dashed line). (C) Epifluorescent composite image of a 12 weeks ob/ob liver with region of indentation from a 1 mm indenter marked with DAPI and stained for lipid accumulation (DAPI, blue; autofluorescence, green; lipid, red). \*indicates an intrahepatic blood vessel within the indented region (white dashed line). Scale bars = 500  $\mu$ m.

ob mice and wild type mice was determined using two-way ANOVA.<sup>30</sup> Statistical significance of the decreasing monotonic trend between increasing local lipid accumulation and local stiffness within sub-mm regions of the ob/ob and wild type mouse liver was determined using Spearman's rank correlation coefficient.<sup>36</sup> Statistical significance of histological metrics was assessed using Student's *t*-test corrected for multiple comparisons using Holm-Sidak. For all statistical analyses, a *P* value of  $\leq 0.05$  was considered significant.

### 3 | RESULTS

#### 3.1 | Simple steatosis is associated with liver softening

To determine the effect of fat accumulation on the solid mechanical properties of the liver without influence from other effects such as variations in perfusion, we compared steatotic and non-steatotic mouse livers *ex vivo* by parallel plate rheometry. We used ob/ob mice as a model of liver steatosis without inflammation or fibrosis, with wild-type littermates as controls. Livers were removed at 8, 12, and 36 weeks of age and showed an increase in lipid droplets in ob/ob mice at all ages compared to controls (Figure 3A,C). Ob/ob mice at 36 weeks of age, however, showed decreased lipid accumulation compared to ob/ob mice at 12 weeks of age. The degree of inflammation was similarly low in ob/ob and control livers (Figure 3D and Figure S1), and picrosirius red staining for collagen showed little to no fibrosis in both ob/ob and control livers at 8 and 12 weeks, with collagen accumulation being lower in ob/ob livers compared to control livers at 36 weeks (Figure 3B,E and Figure S2).

Shear rheometry was performed on liver cores<sup>7</sup> to determine the Young's modulus *E*, showing that livers from ob/ob mice were significantly softer and had less pronounced stiffening under physiologically relevant degrees of compression<sup>30</sup> than those from age-matched controls (Figure 3F). *E* at zero compression was extrapolated from the curve, and was found to be significantly softer in ob/ob mice at 8 and 12 weeks than those from age-matched controls ( $1.50 \pm 0.20$  vs.  $0.98 \pm 0.07$  kPa for 8 weeks and  $2.78 \pm 0.28$  vs.  $1.36 \pm 0.30$  kPa for 12 weeks,  $p < 0.05$  for 8 and 12 weeks by Student's *t*-test). However, there was no significant difference between *E* at zero compression at 36 weeks, when the differences in lipid accumulation were reduced between livers of ob/ob mice and age-matched controls ( $1.59 \pm 0.14$  vs.  $1.09 \pm 0.20$  kPa for 36 weeks, no significance by Student's *t*-test). These results suggest that the degree of steatosis, rather than the duration of steatosis or age, is associated with liver softening.

The liver is subject to shear in addition to compressive forces *in vivo*,<sup>30</sup> and so shear rheometry was used to determine the shear storage modulus *G'* and shear loss modulus *G''* of ob/ob and wild-type liver cores. Although the liver was viscoelastic for all conditions, *G''* was always significantly lower than *G'* and contributed minimally to the complex shear modulus. With the exception of livers at 36 weeks under zero compression or tension, all livers from ob/ob mice had significantly lower moduli and less-pronounced compression stiffening than those from age-matched controls (Figure 4). Thus, *ex vivo* mechanical characterization of ob/ob and wild type mouse livers demonstrates that steatosis is associated with overall liver softening.

#### 3.2 | Association of microindentation with visualization of histological features

Shear rheometry measures the overall mechanics of tissue cores which are millimeters in diameter, and thus is limited to measuring stiffness on the same spatial scale as conventional clinical ultrasound and MRE approaches.<sup>27,28</sup> These measurements do not capture variations in stiffness due to features at the micron scale. For example, fat accumulation is heterogeneous in liver steatosis, preferentially localizing to regions around the central veins.<sup>23</sup> We therefore developed a technique to determine whether localized lipid accumulation is associated with localized softening.

We adapted a previously described *ex vivo* microindentation technique<sup>29</sup> to add the capability of associating cell and tissue structures such as lipid droplets to stiffness measurements within the same submillimeter regions of interest (Figure 1). DAPI was applied to liver cores after maximal indentation, staining around but not under the indenter, resulting in a ring demarcating the region where stiffness was measured. After release of the indenter, whole mount Oil red O staining was used to label lipids. We found that epifluorescence microscopy could be used to simultaneously capture the ring of demarcation by DAPI, lipid accumulation, and liver autofluorescence (Figure 2A,B). Liver autofluorescence was used to avoid measurements over regions with large blood vessels. (Figure 2C).

#### 3.3 | Localized fat accumulation is associated with local softening

We used this adapted microindentation technique to determine the relationship between local lipid accumulation and local stiffness measured *ex vivo* in ob/ob and

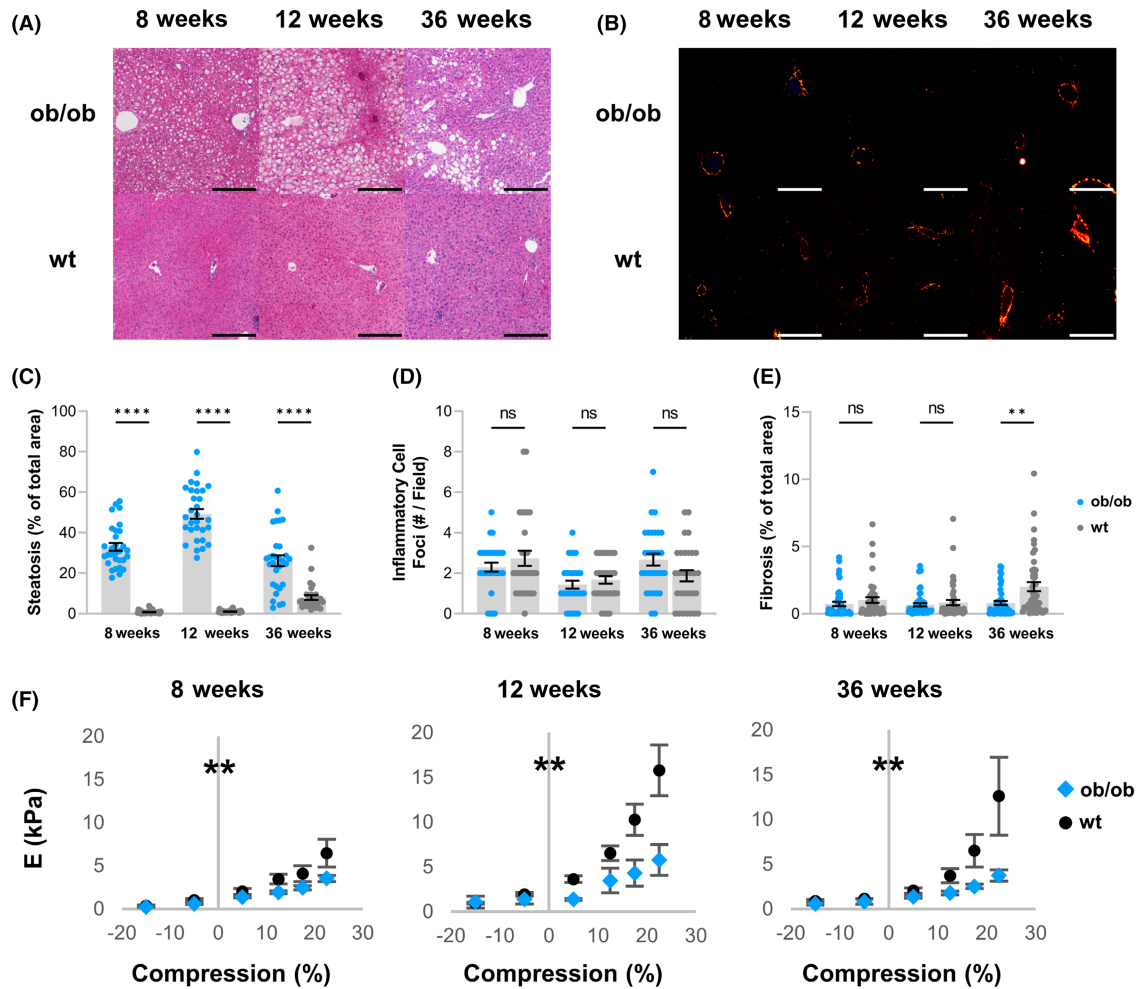


**FIGURE 3** Simple steatosis is associated with lower Young's modulus in ob/ob mice. (A) Representative H&E stains of livers from ob/ob mice and wild type littermates taken at 8, 12, and 36 weeks of age. (B) Representative picrosirius red stains of ob/ob and wt livers taken under polarized light microscopy. Scale bar = 250  $\mu$ m. (C) Steatosis as a percent of total area, (D) frequency of myeloperoxidase (MPO)-positive inflammatory cell foci in 500  $\times$  500  $\mu$ m regions, and (E) fibrosis as a percent of total area of livers from ob/ob mice and wild type littermates taken at 8, 12, and 36 weeks of age.  $n \geq 30$  measurements of regions from three animals for each condition. Error bars indicate standard error. \*\* $p < 0.005$ , and \*\*\*\* $p < 0.00005$  by Student's  $t$ -test. (F) Young's modulus  $E$  of ob/ob (blue) and wt (black) livers at 8, 12, and 36 weeks under varied tension and compression. Ob/ob livers were significantly softer than wt livers.  $n \geq 4$  animals for each condition. Error bars indicate standard error. \*\* $p < 0.005$  for differences between curves by two-way ANOVA.

wild type mouse livers in the absence of other influences such as fluid perfusion. The amount of fat within the demarcated regions was greater in ob/ob livers than controls, and there was marked variation between different demarcated regions in ob/ob livers (Figure 5A). We quantified the amount of lipid staining in the demarcated microindented regions and found a significant inverse correlation between fat content and local stiffness through Spearman's rank correlation across all ages (Figure 5B). The 12 weeks samples, which had the highest lipid accumulation, demonstrated a plateau (percolation threshold) at approximately 50%–60% lipid, beyond which no further softening was observed. Thus, local regions of simple steatosis in rodent livers resulted in associated local softening.

## 4 | DISCUSSION

In this study, we examined the effect of isolated lipid accumulation on liver tissue solid stiffness in the absence of complicating influences in fatty livers such as fibrosis, inflammation, or variations in blood flow.<sup>14,20–22</sup> Using ex vivo approaches to measure the stiffness of steatotic and normal mouse livers at the millimeter and sub-millimeter length scales, we showed that the liver softens substantially in simple steatosis. Furthermore, we developed a technique to visualize local histology in regions of microindentation and used it to demonstrate that the local accumulation of lipid droplets within steatotic livers is associated with local softening. Together, these results show that intrahepatic fat causes liver softening and that

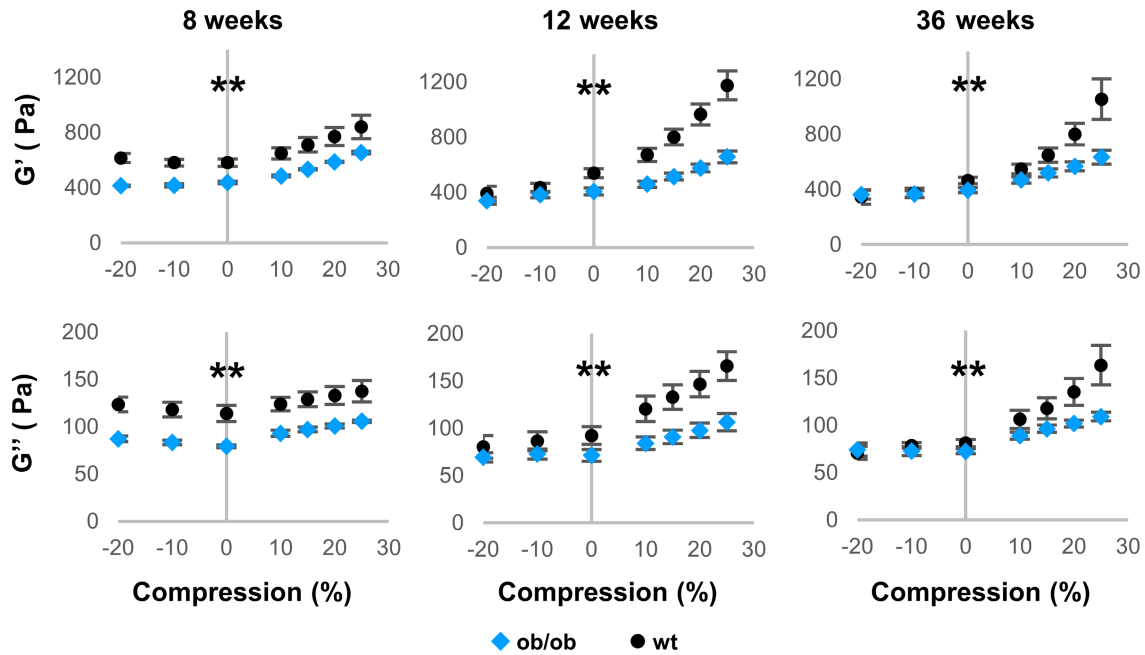


**FIGURE 4** Simple steatosis is associated with lower shear elastic and loss moduli in ob/ob mice. Shear elastic modulus  $G'$  (top) and loss modulus  $G''$  (bottom) of ob/ob (blue) and wt (black) livers at 8, 12, and 36 weeks under varied tension and compression. Ob/ob livers had significantly lower shear elastic and loss moduli than wt livers and less compression stiffening.  $n \geq 4$  animals for each condition. Error bars indicate standard error. \*\* $p < 0.005$  for differences between curves by two-way ANOVA.

its uneven distribution in livers with simple steatosis generates a mechanically heterogeneous environment at the sub-millimeter scale.

A major advantage of this study is the ex vivo characterization of liver mechanics without confounding from perfusion. Liver steatosis can cause decreased liver perfusion<sup>22,37–39</sup> and increased transhepatic pressures<sup>21,40</sup>—both of which can influence measured stiffness in clinical elastography approaches.<sup>20,41</sup> This has led to conflicting literature on whether steatosis softens or stiffens liver tissue during in vivo studies, although recent elastography on patients suggest that livers with simple steatosis are not stiffer and may be softer than normal livers.<sup>42,43</sup> Additionally, changes in stiffness and fluid pressures present different mechanical stimuli to cells, which then cause cells to mount different responses.<sup>44–46</sup> As such, characterizing the stiffness in isolation is important to understanding what stimuli are present in steatosis, and in the development of models to investigate the mechanical role of fat accumulation in fatty liver disease progression.

Steatosis-associated softening at the whole liver level did not automatically mean that steatotic regions would be soft—an alternative hypothesis was that softening occurred preferentially in non-fatty regions of the steatotic liver, possibly due to ECM remodeling.<sup>47</sup> Our new demarcated microindentation-microscopy technique was crucial in determining that localized fat accumulation caused

local softening in the lipid-laden regions. The technique also enabled us to determine that there was a maximum threshold of local fat content at which softening plateaued, as predicted by computational models of systems with two phases of differing mechanical properties.<sup>48,49</sup> The demarcated microindentation-microscopy technique will be applicable to the study of other microarchitectural features in fatty liver disease<sup>23</sup> such as local regions of inflammation or ECM remodeling, as well as studies of microarchitectural and mechanical heterogeneity in other tissue systems and pathologies.

The fat-associated liver softening we observed could result from a variety of biophysical changes in fatty liver tissues and cells. Fat accumulation may induce changes in collagen crosslinking<sup>7</sup> or ECM composition.<sup>30</sup> Changes in the size or number of lipid droplets could also affect the mechanical properties of steatotic cells.<sup>42</sup> Lipid accumulation causes hepatocytes to swell even before ballooning,<sup>50</sup> potentially decreasing stiffness and the compression-stiffening response by reducing the proportion of ECM in a given volume of liver. Additionally, cell membrane area has been hypothesized to contribute to strain stiffening in normal and fibrotic livers by impeding fluid movement and thus hepatocyte swelling may decrease strain stiffening by reducing cell membrane surface area per given volume.<sup>30</sup>

Fat-associated liver softening may have important ramifications for the progression of fatty liver diseases.

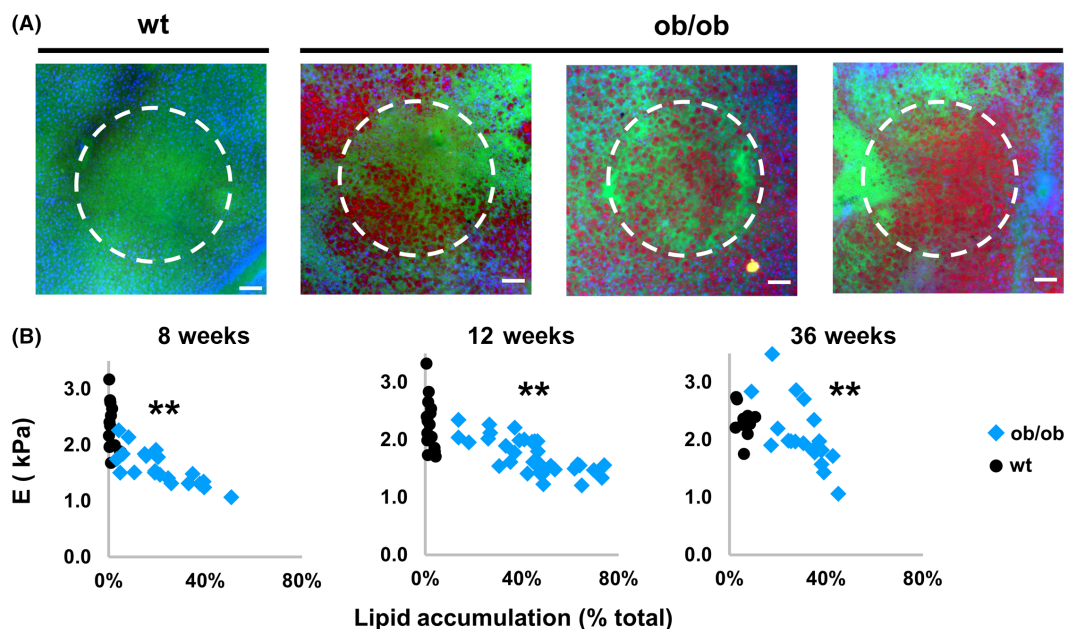


**FIGURE 5** Increased local lipid accumulation in steatosis is associated with local softening. (A) Representative fluorescent images of indented wt and ob/ob livers with increasing lipid accumulation within the indented region, showing DAPI (blue) demarcating the microindented regions (white dashed line), autofluorescence (green), and heterogeneous lipid accumulation using Oil red O (red). Scale bar 100  $\mu\text{m}$ . (B) Scatter plots of Young's modulus  $E$  versus lipid accumulation within microindented regions of ob/ob (blue) and wt (black) livers taken at 8, 12, and 36 weeks. Submillimeter regions of ob/ob livers with greater local steatosis had lower local stiffness at all tested ages.  $n \geq 11$  measurements from  $\geq 3$  animals for each condition.  $**r_s < -0.7$  and  $p < 0.005$  by Spearman's rank correlation.

Changes in substrate stiffness and other mechanical cues influence cell behaviors such as migration, alignment, and ECM remodeling, all of which could play key roles in the response to steatosis and progression to inflammation and fibrosis.<sup>51–53</sup> Additionally, local transitions in and of themselves can serve as mechanical stimuli and cause changes in cell behavior.<sup>25,46,54,55</sup> It is also possible that liver softening exerts a protective effect against potential pro-fibrotic cues such as stiffening from sinusoidal pressure and arterial waves, and thus contributes to the variable stiffness and speed of progression in fatty liver disease.<sup>56</sup>

There are some limitations to this study. All measurements were obtained using a genetic model of simple steatosis, and additional models of simple steatosis such as those from increased dietary sucrose could be studied to determine whether underlying differences in the models result in differences in cell and tissue response.<sup>57</sup> Additionally, the mechanics of the fatty liver in some models might vary as a result of differences in the composition of lipid droplets compared to droplet composition in ob/ob mice.<sup>58</sup>

In summary, we show that fat accumulation is associated with both global and local liver softening, a finding that may have significant implications for understanding the progression of early-stage fatty liver disease. The ability to correlate submillimeter-scale stiffness

measurements with histological features can be used to study the mechanical contributions of microarchitectural changes during the progression of fatty liver disease, and to investigate development and disease in other tissues and organ systems.

#### AUTHOR CONTRIBUTIONS

David Li designed, carried out and analyzed all experiments, wrote the manuscript, and approved the final manuscript. Paul A. Janmey analyzed experiments and reviewed the final manuscript. Rebecca G. Wells conceptualized the project, analyzed data, wrote the manuscript, approved the final manuscript, and obtained funding.

#### ACKNOWLEDGMENTS

The authors thank Jessica Llewellyn, Dongning Chen, Xuechen Shi, and Jeff Byfield for training, technical support, and feedback, the Center for Molecular Studies in Digestive and Liver Diseases (P30DK050306) for histology and microscopy support, Guy Genin for thought-provoking discussions, and Yang Liu for assistance with the illustrations.

#### FUNDING INFORMATION

This work was supported by National Institutes of Health grant R01EB017753 to PAJ and RGW and by the Center

for Engineering MechanoBiology (CEMB), an NSF Science and Technology Center, under grant agreement CMMI1548571.

## DISCLOSURE

The authors declare no conflicts of interest.

## DATA AVAILABILITY STATEMENT

All study data are included in this article and/or supplementary material.

## PREPRINT SERVER

A preprint of this work was published on bioRxiv at <https://doi.org/10.1101/2022.07.14.500092>.

## ORCID

David Li  <https://orcid.org/0000-0002-4285-5598>

Rebecca G. Wells  <https://orcid.org/0000-0002-6988-4102>

## REFERENCES

- Angulo P. Nonalcoholic fatty liver disease. *N Engl J Med*. 2002;346(16):1221-1231. doi:10.1056/NEJMra011775
- Chalasanani N, Younossi Z, Lavine JE, et al. The diagnosis and management of nonalcoholic fatty liver disease: practice guidance from the American Association for the Study of Liver Diseases. *Hepatology*. 2018;67(1):328-357. doi:10.1002/hep.29367
- Younossi ZM, Stepanova M, Younossi Y, et al. Epidemiology of chronic liver diseases in the USA in the past three decades. *Gut*. 2020;69(3):564-568. doi:10.1136/gutjnl-2019-318813
- Theise ND. Histopathology of alcoholic liver disease. *Clin Liver Dis (Hoboken)*. 2013;2(2):64-67. doi:10.1002/cld.172
- Matteoni CA, Younossi ZM, Gramlich T, Boparai N, Liu YC, McCullough AJ. Nonalcoholic fatty liver disease: a spectrum of clinical and pathological severity. *Gastroenterology*. 1999;116(6):1413-1419. doi:10.1016/s0016-5085(99)70506-8
- Georges PC, Hui JJ, Gombos Z, et al. Increased stiffness of the rat liver precedes matrix deposition: implications for fibrosis. *Am J Physiol Gastrointest Liver Physiol*. 2007;293(6):G1147-G1154. doi:10.1152/ajpgi.00032.2007
- Perepelyuk M, Terajima M, Wang AY, et al. Hepatic stellate cells and portal fibroblasts are the major cellular sources of collagens and lysyl oxidases in normal liver and early after injury. *Am J Physiol Gastrointest Liver Physiol*. 2013;304(6):G605-G614. doi:10.1152/ajpgi.00222.2012
- Kostallari E, Wei B, Sicard D, et al. Stiffness is associated with hepatic stellate cell heterogeneity during liver fibrosis. *Am J Physiol Gastrointest Liver Physiol*. 2022;322(2):G234-G246. doi:10.1152/ajpgi.00254.2021
- Shoham N, Girshovitz P, Katzung R, Shaked NT, Benayahu D, Gefen A. Adipocyte stiffness increases with accumulation of lipid droplets. *Biophys J*. 2014;106(6):1421-1431. doi:10.1016/j.bpj.2014.01.045
- Yu H, Tay CY, Leong WS, Tan SC, Liao K, Tan LP. Mechanical behavior of human mesenchymal stem cells during adipogenic and osteogenic differentiation. *Biochem Biophys Res Commun*. 2010;393(1):150-155. doi:10.1016/j.bbrc.2010.01.107
- Labriola NR, Darling EM. Temporal heterogeneity in single-cell gene expression and mechanical properties during adipogenic differentiation. *J Biomech*. 2015;48(6):1058-1066. doi:10.1016/j.jbiomech.2015.01.033
- Abuhattum S, Kotzbeck P, Schlussler R, et al. Adipose cells and tissues soften with lipid accumulation while in diabetes adipose tissue stiffens. *Sci Rep*. 2022;12(1):10325. doi:10.1038/s41598-022-13324-9
- Chin L, Theise ND, Loneker AE, Janmey PA, Wells RG. Lipid droplets disrupt mechanosensing in human hepatocytes. *Am J Physiol Gastrointest Liver Physiol*. 2020;319(1):G11-G22. doi:10.1152/ajpgi.00098.2020
- Mueller S, Millonig G, Sarovska L, et al. Increased liver stiffness in alcoholic liver disease: differentiating fibrosis from steatohepatitis. *World J Gastroenterol*. 2010;16(8):966-972. doi:10.3748/wjg.v16.i8.966
- Wong VW, Vergniol J, Wong GL, et al. Diagnosis of fibrosis and cirrhosis using liver stiffness measurement in nonalcoholic fatty liver disease. *Hepatology*. 2010;51(2):454-462. doi:10.1002/hep.23312
- Gaia S, Carezzi S, Barilli AL, et al. Reliability of transient elastography for the detection of fibrosis in non-alcoholic fatty liver disease and chronic viral hepatitis. *J Hepatol*. 2011;54(1):64-71. doi:10.1016/j.jhep.2010.06.022
- Mouzaki M, Trout AT, Arce-Clachar AC, et al. Assessment of nonalcoholic fatty liver disease progression in children using magnetic resonance imaging. *J Pediatr*. 2018;201:86-92. doi:10.1016/j.jpeds.2018.05.024
- Petta S, Maida M, Macaluso FS, et al. The severity of steatosis influences liver stiffness measurement in patients with nonalcoholic fatty liver disease. *Hepatology*. 2015;62(4):1101-1110. doi:10.1002/hep.27844
- Hudert CA, Tzschatzsch H, Rudolph B, et al. Tomoelastography for the evaluation of pediatric nonalcoholic fatty liver disease. *Invest Radiol*. 2019;54(4):198-203. doi:10.1097/RLI.0000000000000529
- Millonig G, Friedrich S, Adolf S, et al. Liver stiffness is directly influenced by central venous pressure. *J Hepatol*. 2010;52(2):206-210. doi:10.1016/j.jhep.2009.11.018
- Van der Graaff D, Kwanten WJ, Couturier FJ, et al. Severe steatosis induces portal hypertension by systemic arterial hyporeactivity and hepatic vasoconstrictor hyperreactivity in rats. *Lab Invest*. 2018;98(10):1263-1275. doi:10.1038/s41374-017-0018-z
- Davis RP, Surewaard BGJ, Turk M, et al. Optimization of In vivo imaging provides a first look at mouse model of non-alcoholic fatty liver disease (NAFLD) using intravital microscopy. *Front Immunol*. 2019;10:2988. doi:10.3389/fimmu.2019.02988
- Takahashi Y, Fukusato T. Histopathology of nonalcoholic fatty liver disease/nonalcoholic steatohepatitis. *World J Gastroenterol*. 2014;20(42):15539-15548. doi:10.3748/wjg.v20.i42.15539
- Wang H, Abhilash AS, Chen CS, Wells RG, Shenoy VB. Long-range force transmission in fibrous matrices enabled by tension-driven alignment of fibers. *Biophys J*. 2014;107(11):2592-2603. doi:10.1016/j.bpj.2014.09.044
- Wang YL, Li D. Creating complex polyacrylamide hydrogel structures using 3D printing with applications to

- mechanobiology. *Macromol Biosci.* 2020;20(7):e2000082. doi:10.1002/mabi.202000082
26. Stopak D, Harris AK. Connective tissue morphogenesis by fibroblast traction. I tissue culture observations. *Dev Biol.* 1982;90(2):383-398. doi:10.1016/0012-1606(82)90388-8
  27. Sandrin L, Fourquet B, Hasquenoph JM, et al. Transient elastography: a new noninvasive method for assessment of hepatic fibrosis. *Ultrasound Med Biol.* 2003;29(12):1705-1713. doi:10.1016/j.ultrasmedbio.2003.07.001
  28. Wu CH, Ho MC, Jeng YM, et al. Quantification of hepatic steatosis: a comparison of the accuracy among multiple magnetic resonance techniques. *J Gastroenterol Hepatol.* 2014;29(4):807-813. doi:10.1111/jgh.12451
  29. Levental I, Levental KR, Klein EA, et al. A simple indentation device for measuring micrometer-scale tissue stiffness. *J Phys Condens Matter.* 2010;22(19):194120. doi:10.1088/0953-8984/22/19/194120
  30. Perepelyuk M, Chin L, Cao X, et al. Normal and fibrotic rat livers demonstrate shear strain softening and compression stiffening: a model for soft tissue mechanics. *PLoS One.* 2016;11(1):e0146588. doi:10.1371/journal.pone.0146588
  31. Tan K, Cheng S, Juge L, Bilston LE. Characterising soft tissues under large amplitude oscillatory shear and combined loading. *J Biomech.* 2013;46(6):1060-1066. doi:10.1016/j.jbiomech.2013.01.028
  32. de Jong IEM, Bodewes SB, van Leeuwen OB, et al. Restoration of bile duct injury of donor livers during ex situ normothermic machine perfusion. *Transplantation.* 2023. doi:10.1097/TP.0000000000004531
  33. Rensen SS, Slaats Y, Nijhuis J, et al. Increased hepatic myeloperoxidase activity in obese subjects with nonalcoholic steatohepatitis. *Am J Pathol.* 2009;175(4):1473-1482. doi:10.2353/ajpath.2009.080999
  34. Kim SH, Wu SY, Baek JI, et al. A post-developmental genetic screen for zebrafish models of inherited liver disease. *PLoS One.* 2015;10(5):e0125980. doi:10.1371/journal.pone.0125980
  35. Koopman R, Schaart G, Hesslink MK. Optimisation of oil red O staining permits combination with immunofluorescence and automated quantification of lipids. *Histochem Cell Biol.* 2001;116(1):63-68. doi:10.1007/s004180100297
  36. Sunderhauf A, Hicken M, Schlichting H, et al. Loss of mucosal p32/gC1qR/HABP1 triggers energy deficiency and impairs goblet cell differentiation in ulcerative colitis. *Cell Mol Gastroenterol Hepatol.* 2021;12(1):229-250. doi:10.1016/j.jcmgh.2021.01.017
  37. Seifalian AM, Chidambaram V, Rolles K, Davidson BR. In vivo demonstration of impaired microcirculation in steatotic human liver grafts. *Liver Transpl Surg.* 1998;4(1):71-77. doi:10.1002/lt.500040110
  38. Farrell GC, Teoh NC, McCuskey RS. Hepatic microcirculation in fatty liver disease. *Anat Rec (Hoboken).* 2008;291(6):684-692. doi:10.1002/ar.20715
  39. McCuskey RS, Ito Y, Robertson GR, McCuskey MK, Perry M, Farrell GC. Hepatic microvascular dysfunction during evolution of dietary steatohepatitis in mice. *Hepatology.* 2004;40(2):386-393. doi:10.1002/hep.20302
  40. van der Graaff D, Chotkoe S, De Winter B, et al. Vasoconstrictor antagonism improves functional and structural vascular alterations and liver damage in rats with early NAFLD. *JHEP Rep.* 2022;4(2):100412. doi:10.1016/j.jhepr.2021.100412
  41. Tang A, Cloutier G, Szeverenyi NM, Sirlin CB. Ultrasound elastography and MR elastography for assessing liver fibrosis: part 2, diagnostic performance, confounders, and future directions. *AJR Am J Roentgenol.* 2015;205(1):33-40. doi:10.2214/AJR.15.14553
  42. Mueller S, Lackner C. Histological confounders of liver stiffness. In: Mueller S, ed. *Liver Elastography: Clinical Use and Interpretation.* 1st ed. Springer International Publishing; 2020:233-242.
  43. Karlas T, Mueller S. Liver steatosis (CAP) as modifier of liver stiffness. In: Mueller S, ed. *Liver Elastography: Clinical Use and Interpretation.* 1st ed. Springer International Publishing; 2020:459-467.
  44. Olsen AL, Bloomer SA, Chan EP, et al. Hepatic stellate cells require a stiff environment for myofibroblastic differentiation. *Am J Physiol Gastrointest Liver Physiol.* 2011;301(1):G110-G118. doi:10.1152/ajpgi.00412.2010
  45. Qi F, Hu JF, Liu BH, et al. MiR-9a-5p regulates proliferation and migration of hepatic stellate cells under pressure through inhibition of Sirt1. *World J Gastroenterol.* 2015;21(34):9900-9915. doi:10.3748/wjg.v21.i34.9900
  46. Moriyama K, Kidoaki S. Cellular Durotaxis revisited: initial-position-dependent determination of the threshold stiffness gradient to induce Durotaxis. *Langmuir.* 2019;35(23):7478-7486. doi:10.1021/acs.langmuir.8b02529
  47. Kisseleva T, Brenner D. Molecular and cellular mechanisms of liver fibrosis and its regression. *Nat Rev Gastroenterol Hepatol.* 2021;18(3):151-166. doi:10.1038/s41575-020-00372-7
  48. Chen Y, Schuh CA. Elasticity of random multiphase materials: percolation of the stiffness tensor. *Journal of Statistical Physics.* 2016;162(1):232-241. doi:10.1007/s10955-015-1387-6
  49. Kantor Y, Webman I. Elastic properties of random percolating systems. *Physical Review Letters.* 1984;52(21):1891-1894. doi:10.1103/PhysRevLett.52.1891
  50. Hall A, Covelli C, Manuguerra R, et al. Transaminase abnormalities and adaptations of the liver lobule manifest at specific cut-offs of steatosis. *Sci Rep.* 2017;7:40977. doi:10.1038/srep40977
  51. Desai SS, Tung JC, Zhou VX, et al. Physiological ranges of matrix rigidity modulate primary mouse hepatocyte function in part through hepatocyte nuclear factor 4 alpha. *Hepatology.* 2016;64(1):261-275. doi:10.1002/hep.28450
  52. Wells RG. The role of matrix stiffness in regulating cell behavior. *Hepatology.* 2008;47(4):1394-1400. doi:10.1002/hep.22193
  53. Discher DE, Janmey P, Wang YL. Tissue cells feel and respond to the stiffness of their substrate. *Science.* 2005;310(5751):1139-1143. doi:10.1126/science.1116995
  54. Lo CM, Wang HB, Dembo M, Wang YL. Cell movement is guided by the rigidity of the substrate. *Biophys J.* 2000;79(1):144-152. doi:10.1016/S0006-3495(00)76279-5
  55. Lachowski D, Cortes E, Robinson B, Rice A, Rombouts K, Del Rio Hernandez AE. FAK controls the mechanical activation of YAP, a transcriptional regulator required for durotaxis. *FASEB J.* 2018;32(2):1099-1107. doi:10.1096/fj.201700721R
  56. Mueller S. Does pressure cause liver cirrhosis? The sinusoidal pressure hypothesis. *World J Gastroenterol.* 2016;22(48):10482-10501. doi:10.3748/wjg.v22.i48.10482
  57. Song Z, Deaciuc I, Zhou Z, et al. Involvement of AMP-activated protein kinase in beneficial effects of betaine on high-sucrose diet-induced hepatic steatosis. *Am J Physiol Gastrointest Liver Physiol.* 2007;293(4):G894-G902. doi:10.1152/ajpgi.00133.2007

58. Thiam AR, Farese RV Jr, Walther TC. The biophysics and cell biology of lipid droplets. *Nat Rev Mol Cell Biol.* 2013;14(12):775-786. doi:10.1038/nrm3699

### SUPPORTING INFORMATION

Additional supporting information can be found online in the Supporting Information section at the end of this article.

**How to cite this article:** Li D, Janmey PA, Wells RG. Local fat content determines global and local stiffness in livers with simple steatosis. *FASEB BioAdvances.* 2023;5:251-261. doi:10.1096/fba.2022-00134